

# Important role of the spin-orbit interaction in forming the $1/2^+$ orbital structure in Be isotopes

*N. Itagaki, S. Okabe\*, and K. Ikeda*

*RI Beam Science Laboratory, RIKEN (The Institute of Physical and Chemical Research),  
Wako, Saitama 351-0198, Japan*

*\* Center for Information and Multimedia Studies, Hokkaido University,  
Sapporo 060-0810, Japan*

## Abstract

The structure of the second  $0^+$  state of  $^{10}\text{Be}$  is investigated using a microscopic  $\alpha+\alpha+n+n$  model based on the molecular-orbit (MO) model. The second  $0^+$  state, which has dominantly the  $(1/2^+)^2$  configuration, is shown to have a particularly enlarged  $\alpha$ - $\alpha$  structure. The kinetic energy of the two valence neutrons occupying along the  $\alpha$ - $\alpha$  axis is reduced remarkably due to the strong  $\alpha$  clustering and, simultaneously, the spin-orbit interaction unexpectedly plays important role to make the energy of this state much lower. The mixing of states with different spin structure is shown to be important in negative-parity states. The experimentally observed small-level spacing between  $1^-$  and  $2^-$  ( $\sim 300$  keV) is found to be an evidence of this spin-mixing effect.  $^{12}\text{Be}$  is also investigated using  $\alpha+\alpha+4n$  model, in which four valence neutrons are considered to occupy the  $(3/2^-)^2(1/2^+)^2$  configuration. The energy surface of  $^{12}\text{Be}$  is shown to exhibit similar characteristics, that the remarkable  $\alpha$  clustering and the contribution of the spin-orbit interaction make the binding of the state with  $(3/2^-)^2(1/2^+)^2$  configuration properly stronger in comparison with the closed  $p$ -shell  $(3/2^-)^2(1/2^-)^2$  configuration.

PACS number(s): 21.10.-k, 21.60.Gx

## I. INTRODUCTION

Numerous experiments using unstable nuclear beams have succeeded to reveal exotic properties of  $\beta$ -unstable nuclei, including a neutron halo structure [1–3]. Especially, the shift of the closed-shell structure is a characteristic behavior of systems with weakly bound neutrons. Recently, the contributions of the  $sd$  shell have been analyzed in  $N = 8$  nuclei based on the shell model. A calculation has shown that the slow  $\beta$ -decay of  $^{12}\text{Be}$  to  $^{12}\text{B}$  can be explained by an admixture of the  $sd$  shell in  $^{12}\text{Be}$  ( $N = 8$ ) in which the closed  $p$ -shell component must be less than 30% [4]. This shows that the concept of magic numbers is vague in  $^{12}\text{Be}$ .

On the other hand, an  $\alpha$ - $\alpha$  structure is well established in the Be and B region. Typically in  $^9\text{Be}$ , a microscopic  $\alpha+\alpha+n$  model has reproduced the properties of low-lying states

including the level inversion of  $1/2^-$  in the  $p$ -shell and  $1/2^+$  in the  $sd$  shell [5,6]. Also in  $^{10}\text{Be}$ , the microscopic  $\alpha$ -cluster models have been applied [7,8], and we have quantitatively shown the mechanism for the lowering of the  $sd$  orbits related with the clustering of the core [9].

According to our previous results for  $^{10}\text{Be}$ , the main properties of this nucleus have been well described by the  $\alpha+\alpha+n+n$  model, where the orbits for the two valence neutrons are classified based on the molecular-orbit (MO) model. The dominant configuration of the two valence neutrons for the second  $0^+$  state is  $(1/2^+)^2$ , and the level inversion between  $1/2^-$  and  $1/2^+$  in  $^9\text{Be}$  also holds in  $^{10}\text{Be}$ . Here, the two valence neutrons stay along the  $\alpha$ - $\alpha$  axis, and reduce the kinetic energy by enhancing the  $\alpha$ - $\alpha$  distance (up to around 4 fm). Therefore, the  $1/2^+$  orbit in this case is not a spherical  $s$ -wave, but a polarized orbit with the  $d$ -wave component. This feature of  $sd$  mixing in the  $1/2^+$  orbit can be qualitatively interpreted in terms of deformed models ([220] expression in the Nilsson diagram).

The main purpose of this paper is to show the mechanism for the appearance of this  $(1/2^+)^2$  configuration in low-lying energy in detail. In our previous work, the calculated excitation energy of the second  $0^+$  state has been higher by  $\sim 5$  MeV without the spin-orbit interaction than the experimental one [9]. The spin-orbit interaction has been found to decrease the excitation energy by 3 MeV by adding a single optimal wave function with  $S = 1$ . Hence, it is necessary to analyze the contribution of the spin-orbit interaction more precisely to clarify the lowering mechanism of the second  $0^+$  state. The other reduction mechanism of the kinetic energy by more accurate description of the neutron-tail should also be taken into account.

Firstly, the spin-orbit interaction is able to contribute to the second  $0^+$  state, when spin-triplet states for the valence neutrons are included among the basis states. If the  $1/2^+$  state consists of the pure  $s$ -orbit, naturally there is no contribution of the spin-orbit interaction. In Be isotopes, the state contains the  $d$ -orbit component. However, the spin-orbit interaction again vanishes, when the two valence neutrons occupy along the  $\alpha$ - $\alpha$  axis, since two neutrons with the same spatial distribution construct only the spin-singlet state. This has been the situation in traditional MO models [7,8]. It will be shown that when one of the valence neutrons deviates from the  $\alpha$ - $\alpha$  axis, the spin-triplet state can be constructed, and the spin-orbit interaction strongly acts between this state and the original  $(1/2^+)^2$  configuration with the spin-singlet. The extension of the model space also enables us to improve the description of the neutron-tail. We estimate the reduction of the kinetic energy due to the improvement of the neutron-tail. These improvements will be shown to largely decrease the excitation energy of the second  $0^+$  state, and that the calculated energy just corresponds to the experimental value.

Using the present extended MO model, negative-parity states in  $^{10}\text{Be}$  are also investigated. The mixing of different spin structure ( $S = 0, S = 1$ ) is found to also be important in the negative-parity states. The  $K$ -mixing effect strongly acts on the  $2^-$  state, and the calculated small-level spacing between  $1^-$  and  $2^-$  ( $\sim 300$  keV) agrees with the experimental value.

Also, in  $^{12}\text{Be}$  these two important mechanism for lowering the  $(1/2^+)^2$  configuration are examined. In  $^{12}\text{Be}$ , the configuration for four valence neutrons around the  $\alpha$ - $\alpha$  core is considered to correspond to the two pair configurations,  $(3/2^-)^2$  and  $(1/2^+)^2$ . These two pair configurations appear in the ground  $0^+$  state and the second  $0^+$  state of  $^{10}\text{Be}$ , respectively.

The energy surface for the ground state of  $^{12}\text{Be}$  will be shown, in which the spin-orbit interaction is seen to make the binding for the  $(3/2^-)^2(1/2^+)^2$  configuration properly stronger in comparison with the  $(3/2^-)^2(1/2^-)^2$  configuration. This is related to the breaking of the  $N = 8$  (closed  $p$ -shell) neutron-magic number.

This paper is organized as follows. In Sec. II, we summarize a description of the single-particle orbits around the two  $\alpha$  clusters based on the MO model. In Sec. III, the contribution of the spin-orbit interaction to the  $(1/2^+)^2$  configuration and the reduction of the kinetic energy due to an improvement of the neutron-tail are considered. These effects are discussed in detail for the second  $0^+$  state of  $^{10}\text{Be}$  (**A**), for the negative parity states of  $^{10}\text{Be}$  (**B**), and for  $^{12}\text{Be}$  (**C**). The conclusion is given in Sec. IV.

## II. EXTENDED MOLECULAR ORBITAL MODEL

We introduce a microscopic  $\alpha+\alpha+2n$  model for  $^{10}\text{Be}$  and  $\alpha+\alpha+4n$  model for  $^{12}\text{Be}$ . The neutron configurations are classified according to the molecular-orbit (MO) picture [10]. The details of the framework are given in Ref. [9]; here, the essential part is presented.

The Hamiltonian is the same as in Ref. [9], and consists of a kinetic-energy term, a central two-body interaction term, a two-body spin-orbit interaction term, and a Coulomb interaction term:

$$\mathcal{H} = \sum_i T_i - T_{cm} + \sum_{i<j} V_{ij} + \sum_{i<j} V_{ij}^{ls} + \sum_{i<j} \frac{e^2}{4r_{ij}} (1 - \tau_z^i)(1 - \tau_z^j). \quad (1)$$

The effective nucleon-nucleon interaction is Volkov No.2 [11] for the central part and the G3RS spin-orbit term [12] for the spin-orbit part, as follows:

$$V_{ij} = \{V_1 e^{-a_1 r_{ij}^2} - V_2 e^{-a_2 r_{ij}^2}\} \{W - MP^\sigma P^\tau + BP^\sigma - HP^\tau\}, \quad (2)$$

$$V_{ij}^{ls} = V_0^{ls} \{e^{-a_1 r_{ij}^2} - e^{-a_2 r_{ij}^2}\} \vec{L} \cdot \vec{S} P_{31}, \quad (3)$$

where  $P_{31}$  is a projection operator onto the triplet odd state. The parameters are  $V_1 = -60.650$  MeV,  $V_2 = 61.140$  MeV,  $a_1 = 0.980$  fm $^{-2}$  and  $a_2 = 0.309$  fm $^{-2}$  for the central interaction, and  $V_0^{ls} = 2000$  MeV,  $a_1 = 5.00$  fm $^{-2}$ , and  $a_2 = 2.778$  fm $^{-2}$  for the spin-orbit interaction. We employ the Majorana exchange parameter,  $M = 0.6$  ( $W = 0.4$ ), the Bartlett exchange parameter,  $B = 0.125$ , and the Heisenberg exchange parameter,  $H = 0.125$ , for the Volkov interaction (using  $B$  and  $H$ , there is no neutron-neutron bound state). All of these parameters are determined from the  $\alpha + n$  and  $\alpha + \alpha$  scattering phase shifts and the binding energy of the deuteron [6].

The total wave function is fully antisymmetrized and expressed by a superposition of terms centered to different relative distances between the two  $\alpha$  clusters ( $d$ ) with various configurations of the valence neutrons. The projection to the eigen-states of angular momentum ( $J$ ) is performed numerically. All nucleons are described by Gaussians with the oscillator parameter ( $s$ ) equal to 1.46 fm. The  $\alpha$  clusters located at  $d/2$  and  $-d/2$  on the  $z$ -axis consist of four nucleons:

$$\phi^{(\alpha)} = G_{R\alpha}^{p\uparrow} G_{R\alpha}^{p\downarrow} G_{R\alpha}^{n\uparrow} G_{R\alpha}^{n\downarrow} \chi_{p\uparrow} \chi_{p\downarrow} \chi_{n\uparrow} \chi_{n\downarrow}. \quad (4)$$

$G$  represents Gaussians:

$$G_{R_\alpha} = \left(\frac{2\nu}{\pi}\right)^{\frac{3}{4}} \exp[-\nu(\vec{r} - \vec{R}_\alpha)^2], \quad \nu = 1/2s^2, \quad \vec{R}_\alpha = \{d\vec{e}_z/2, -d\vec{e}_z/2\}. \quad (5)$$

Each valence neutron ( $\phi_{ci}\chi_{ci}$ ) around the  $\alpha$ - $\alpha$  core is expressed by a linear combination of local Gaussians:

$$\phi_{ci}\chi_{ci} = \sum_j g_j G_{R_n^j} \chi_{ci}, \quad (6)$$

$$G_{R_n^j} = \left(\frac{2\nu}{\pi}\right)^{\frac{3}{4}} \exp[-\nu(\vec{r} - \vec{R}_n^j)^2], \quad \nu = 1/2s^2. \quad (7)$$

The level structure is solved by superposing basis states with different  $\alpha$ - $\alpha$  distances and configurations after the angular momentum projection.

In the MO model, valence neutrons are expressed by a linear combination of orbits around two  $\alpha$  clusters. The orbit around each  $\alpha$  cluster is called the atomic orbit (AO). Here, we note that the valence neutrons and neutrons in the  $\alpha$  clusters are identical particles, and antisymmetrization imposes the AO forbidden space. The lowest AO has one node and parity minus, which is the  $p$ -orbit. When a linear combination of two AOs ( $p$ -orbit) around the left- $\alpha$  cluster and the right- $\alpha$  cluster is summed up by the same sign, the resultant MO also has negative parity and one node. In this case, the MO is restricted to spread along an axis perpendicular to the  $\alpha$ - $\alpha$  ( $z$ ) axis, which is the so-called  $\pi$ -orbit. It cannot spread along the  $z$ -axis where the two  $\alpha$  clusters are already located. If two  $p$ -orbits are summed up by different signs, the resultant MO has two nodes and positive parity. This MO can spread to all directions, and the optimal direction becomes the  $z$ -direction. This is the so-called  $\sigma$ -orbit, and the energy becomes lower as the distance between two  $\alpha$  clusters increases.

In Be isotopes, the low-lying orbits with  $K^\pi = 3/2^-, 1/2^+$ , and  $1/2^-$  are important; these are classified based on the MO model. The  $1/2^+$  state is the  $\sigma$ -orbit, and the spin-orbit interaction splits the  $\pi$ -orbit to  $3/2^-$  and  $1/2^-$ . In the present framework, each valence neutron is introduced to have a definite  $K^\pi$  at the zero limit of centers of local Gaussians ( $\{R_n^j\}$ ) describing the spatial distribution of the orbit. The precise positions of  $\{R_n^j\}$  are determined variationally for each  $\alpha$ - $\alpha$  distance before the angular-momentum projection. Since the values of  $\{R_n^j\}$  are optimized to be finite, the orbits are not exactly the eigen-state of  $K^\pi$ , and are labeled as  $\bar{K}^\pi$ .

In  $^{10}\text{Be}$ , when two valence neutrons occupy these single particle orbits, three configurations with the total  $\bar{K} = \bar{K}_1 + \bar{K}_2 = 0$  are generated. For the ground state, valence neutrons occupy orbits with  $\bar{K}^\pi = 3/2^-$  and  $\bar{K}^\pi = -3/2^-$ ; these  $\pi$ -orbits are expressed as linear combinations of  $p_x$  and  $p_y$ :

$$\Phi(3/2^-, -3/2^-) = \mathcal{A}[\phi_1^{(\alpha)}\phi_2^{(\alpha)}(\phi_{c1}\chi_{c1})(\phi_{c2}\chi_{c2})]. \quad (8)$$

$$\phi_{c1}\chi_{c1} = \{(p_x + ip_y)_{+a} + (p_x + ip_y)_{-a}\}|n \uparrow\rangle, \quad (9)$$

$$\phi_{c2}\chi_{c2} = \{(p_x - ip_y)_{+a} + (p_x - ip_y)_{-a}\}|n \downarrow\rangle. \quad (10)$$

Each MO is constructed from two AOs around a left and right  $\alpha$  cluster. We introduce a variational parameter ( $a$ ) on the  $\alpha$ - $\alpha$  axis ( $z$ -axis); and  $(p_x \pm ip_y)_{+a}$  is  $p_x \pm ip_y$ , whose center is  $+a$  on the  $z$ -axis; and  $(p_x \pm ip_y)_{-a}$  is  $p_x \pm ip_y$ , whose center is  $-a$  on the  $z$ -axis. Here, the spatial part and the spin part of  $\bar{K}$  in Eqs. (9) and (10) are introduced to be parallel, for which the spin-orbit interaction acts attractively. The spin-up valence neutron has  $\bar{K}_1^\pi = 3/2^- (rY_{11}|n \uparrow)$ , and the spin-down valence neutron has  $\bar{K}_1^\pi = 3/2^- (rY_{1-1}|n \downarrow)$ . There  $(p_x)_{+a}$ ,  $(p_x)_{-a}$ ,  $(p_y)_{+a}$ , and  $(p_y)_{-a}$  are expressed as the combination of two Gaussians, whose centers are shifted by a variational parameter ( $b$ ) perpendicular to the  $z$ -axis. For example,

$$(p_x)_{+a} = G_{a\vec{e}_z+b\vec{e}_x} - G_{a\vec{e}_z-b\vec{e}_x}, \quad (p_y)_{+a} = G_{a\vec{e}_z+b\vec{e}_y} - G_{a\vec{e}_z-b\vec{e}_y}. \quad (11)$$

These parameters  $a$  and  $b$ , are optimized by using the Cooling Method in antisymmetrized molecular dynamics (AMD) [13–17] for each  $\alpha$ - $\alpha$  distance.

The  $\sigma$ -orbit pair,  $(1/2^+)^2$ , is prepared, where each  $\sigma$ -orbit is expressed by subtracting two AOs at  $+a = d/2$  and  $-a = -d/2$ :

$$\Phi(1/2^+, -1/2^+) = \mathcal{A}[\phi_1^{(\alpha)}\phi_2^{(\alpha)}(\phi_{c1}\chi_{c1})(\phi_{c2}\chi_{c2})], \quad (12)$$

$$\phi_{c1}\chi_{c1} = \{(\vec{p})_{+a} - (\vec{p})_{-a}\}|n \uparrow\} \quad a = d/2, \quad (13)$$

$$\phi_{c2}\chi_{c2} = \{(\vec{p})_{+a} - (\vec{p})_{-a}\}|n \downarrow\} \quad a = d/2, \quad (14)$$

where,

$$(\vec{p})_{\pm a} = (G_{+\vec{b}} - G_{-\vec{b}})_{\pm a}. \quad (15)$$

Since the  $\sigma$ -orbit has two nodes, the direction of the orbit is not limited due to the Pauli principle. It can thus take all directions. Therefore, the direction and value of parameter  $\vec{b}$  for the center of the Gaussians are optimized. As a result, it is optimized to the direction of the  $\alpha$ - $\alpha$  axis. This basis state shares the dominant component of the second  $0^+$  state.

### III. RESULTS OBTAINED USING THE EXTENDED MO MODEL SPACE

#### A. $J^\pi = 0^+$ states in $^{10}\text{Be}$

Before giving the results, we summarize the calculated energies and the optimal  $\alpha$ - $\alpha$  distance for three configurations ( $(3/2^-)^2$ ,  $(1/2^-)^2$ , and  $(1/2^+)^2$ ) discussed in Ref. [9]. In Fig. 1, the  $0^+$  energy curves of  $\Phi(3/2^-, -3/2^-)$ ,  $\Phi(1/2^+, -1/2^+)$ , and  $\Phi(1/2^-, -1/2^-)$  in  $^{10}\text{Be}$  are presented as a function of the  $\alpha$ - $\alpha$  distance ( $d$ ). These configurations are the dominant components of the first, second, and third  $0^+$  states in  $^{10}\text{Be}$ , respectively.

---

Fig. 1

---

The energy of  $\Phi(1/2^+, -1/2^+)$  (dominant component of  $0_2^+$ ) becomes lower as  $d$  increases, and the energy becomes minimum at an  $\alpha$ - $\alpha$  distance of  $4 \sim 5$  fm. However, it should be noted that the energy difference between  $\Phi(1/2^+, -1/2^+)$  and  $\Phi(3/2^-, -3/2^-)$  in Fig. 1 is about 11 MeV. This is much larger than the experimental excitation energy of the second  $0^+$  state (6.26 MeV [18]) by 5 MeV.

There are two reasons for this lack of binding energy by 5 MeV in the second  $0^+$  state. One is that the contribution of the spin-orbit interaction is not taken into account; the other is that the tail of the valence neutron is not correctly described. As for the spin-orbit interaction, in the traditional MO model, the spin-orbit interaction has not contributed to the  $0^+$  state with this configuration. This is because, the two valence neutrons occupy the same spatial configurations with opposite spin direction, and construct a spin-singlet state. Since it is impossible for two valence neutrons with the same spin direction to occupy the same  $\sigma$ -orbit along the  $\alpha$ - $\alpha$  axis, the spin-triplet state is prepared by making one of the valence neutrons deviate from the  $\alpha$ - $\alpha$  axis. As for the tail effect of the valence neutrons, in this analysis, the tail behavior is expressed by the superposition of local Gaussians.

These two improvements are shown for the  $\Phi(1/2^+, -1/2^+)$  configuration with the optimal  $\alpha$ - $\alpha$  distance of 4 fm. The optimized parameter  $\vec{b}$  is  $2.02\vec{e}_z$  (fm) [9]. As listed in Table I, the spin-singlet  $\Phi(1/2^+, -1/2^+)$  configuration has a  $0^+$  energy of  $-46.3$  MeV. As shown in Eqs. (12)-(15), each valence neutron is described as a linear combination of four local Gaussians. When we optimize their linear combination, the energy slightly decreases to  $-47.7$  MeV (noted as  $S = 0$  ( $\sigma$ )<sup>2</sup> in Table I).

---

Table I

---

Next, the contribution of the spin-orbit interaction is taken into account to this spin-singlet state by preparing the spin-triplet state ( $S_z = 1$ ). One of the valence neutrons ( $\phi_{c1}\chi_{c1}$ ) occupies the  $\sigma$ -orbit, and another one ( $\phi_{c2}\chi_{c2}$ ) with the same spin-direction deviates from the  $\alpha$ - $\alpha$  axis. The later one is described by a local Gaussian centered at  $\vec{R}$ ;  $\phi_{c2}\chi_{c2} = G_{\vec{R}}|n \uparrow\rangle$ . The calculated energy surface for the second  $0^+$  state as a function of the parameter  $\vec{R}$  is given in Fig. 2. The orthogonality of the ground  $0^+$  state to the ground  $0^+$  state is ensured in this calculation. The point on the  $x$ - $z$  plain in Fig. 2 shows the position of the parameter  $\vec{R}$ , and the contour map shows the total energy obtained by taking into account this coupling with the spin-triplet states.

---

Fig. 2

---

The lowest energy of  $-50.9$  MeV is seen at  $\vec{R} = (x, z) = (1.0, 2.0)$  (fm) on the energy surface. The contribution of the spin-orbit interaction decreases the energy by more than 3 MeV in comparison with the case of the spin-singlet state. Although the energy of such a spin-triplet state, itself, is much higher than that of  $\Phi(1/2^+, -1/2^+)$  by about 20 MeV, the large coupling between the spin-singlet and spin-triplet states enables the spin-orbit interaction to attractively act. As a result, more than half of the under-binding by 5 MeV for the second  $0^+$  state is explained by this spin-orbit contribution.

To see this effect more correctly, a lot of spin-triplet states with different  $\vec{R}$  values are adopted. The employed  $\vec{R}$  values are 0.0, 1.0, 2.0 (fm) for the  $x$ -direction (perpendicular to the  $\alpha$ - $\alpha$  direction) and 0.0, 1.0, 2.0, 3.0, 4.0 (fm) for the  $z$ -direction (the  $\alpha$ - $\alpha$  direction). In Table I, the column noted as spin-orbit gives the energy of the second  $0^+$  state when these 15 spin-triplet states with different  $\vec{R}$  values are superposed. The calculated energy is  $-51.2$  MeV; this is lower than the energy minimum point in Fig. 2 by only 300 keV. This is because, the spin-triplet basis states around the core have a large overlap with each other, and those apart from the core do not contribute to this coupling. This result shows that the contribution of the spin-orbit interaction for the  $(1/2^+)^2$  state is approximately taken into account when we employ only one Slater determinant on the energy surface.

In this calculation, many spin-triplet states are employed; however, it should be noted that the spin-singlet state is only represented by the  $\Phi(1/2^+, -1/2^+)$  configuration. Thus, to improve the tail of the valence neutron in the second  $0^+$  state of  $^{10}\text{Be}$ , it is necessary to superpose further the  $S_z = 0$  basis states with many different  $\vec{R}$  values, which contain the spin-singlet component. The distance of  $\alpha$ - $\alpha$  is 4 fm, where one of the valence neutrons ( $\phi_{c1}\chi_{c1}$ ) occupies the  $\sigma$ -orbit, and the other valence neutrons ( $\phi_{c2}\chi_{c2}$ ) with the opposite spin-direction is described by local Gaussian centered at  $\vec{R}$ . The later one has the form of  $\phi_{c2}\chi_{c2} = G_{\vec{R}}|n \downarrow\rangle$ . We superpose 15 basis states with  $S_z = 0$ , and the employed  $\vec{R}$  values are 0.0, 1.0, 2.0 (fm) for the  $x$ -direction (perpendicular to the  $\alpha$ - $\alpha$  direction) and 0.0, 1.0, 2.0, 3.0, 4.0 (fm) for the  $z$ -direction (the  $\alpha$ - $\alpha$  direction). As listed in Table I, the energy becomes  $-52.7$  MeV. These basis states increase the binding of the second  $0^+$  state by 1.5 MeV compared with  $-51.2$  MeV for the third row. Here, it is noted that these  $S_z = 0$  basis states contain both the spin-single and spin-triplet components. However, the increase of the binding energy by adding these  $S_z = 0$  basis states is due to the spin-singlet basis states, since it is considered that the functional space of the spin-triplet states are already exhausted by the  $S_z = 1$  states. These results show that by taking into account both the spin-orbit interaction (spin-triplet basis states) and the tail effect (spin-singlet basis states), the under-binding for the second  $0^+$  state by 5 MeV is fully explained. The calculated excitation energy of the second  $0^+$  state agrees with the experimental one.

To confirm the component of the spin-triplet configurations introduced, the expectation value of the spin-square ( $\hat{S}^2$ ) in the second  $0^+$  state of  $^{10}\text{Be}$  was calculated. The value is 0.26. This means that the spin-triplet configuration mixes in this state by about 13%.

In this analysis, the  $\alpha$ - $\alpha$  distance is restricted to 4 fm, but we now examine the contribution of the spin-orbit interaction with respect to the  $\alpha$ - $\alpha$  distance.

---

Table II

---

Table II gives the contribution of spin-orbit interaction for the second  $0^+$  state with the  $\alpha$ - $\alpha$  distance of 3 fm, 4 fm, and 5 fm. The column noted as  $S = 0$  ( $\sigma$ )<sup>2</sup> gives the energy for the  $\Phi(1/2^+, -1/2^+)$  configuration, where the linear combination of Gaussians is optimized. The column noted as  $+S_z = 1$  gives the energy when we include the spin-orbit interaction by employing the spin-triplet basis states. The results show that the smaller is the  $\alpha$ - $\alpha$  distance, the larger is the contribution of the coupling with the spin-triplet state. When the  $\alpha$ - $\alpha$  distance is 5 fm, the coupling increases the binding energy by about 3 MeV; however,

when the  $\alpha$ - $\alpha$  distance is 3 fm, the coupling increases the binding energy by about 4.5 MeV. Therefore, the coupling with the spin-triplet becomes stronger as the  $\alpha$ - $\alpha$  distance becomes small. The column noted as  $+S_z = 0, 1$  gives the energy when we further include the spin-singlet basis state to express the tail of the valence neutron. This effect does not have a strong dependence on the  $\alpha$ - $\alpha$  distance, and almost constantly decreases the binding energy by 1.5 MeV.

Finally, the calculation where all of these basis states with different  $\alpha$ - $\alpha$  distance are superposed is performed based on the generator coordinate method (GCM). When we superpose all of the basis states in Table II, the calculated energy of the second  $0^+$  state becomes  $-54.3$  MeV. Here, we superpose the basis states with  $\alpha$ - $\alpha$  distances of 3, 4, 5, and 6 fm, and the spin-triplet states are represented by one Slater determinant for each  $\alpha$ - $\alpha$  distance, which correspond to the minimum point on the energy surface (Fig. 2). This calculated energy of  $-54.3$  MeV is lower than a result calculated with only the  $\Phi(1/2^+, -1/2^+)$  configuration (employed  $\alpha$ - $\alpha$  distances are the same) by 4.6 MeV.

## B. Negative-parity states in $^{10}\text{Be}$

We examine this spin-mixing effect for the negative-parity states in  $^{10}\text{Be}$ . Here, one of the valence neutrons is introduced to occupy a  $\pi$ -orbit with negative parity; another one occupies a  $\sigma$ -orbit with positive parity. In this way, two configurations with  $S_z = 0$  and  $S_z = 1$  can be constructed. The  $S_z = 0$  basis state ( $\Phi(3/2^-, -1/2^+)$ ) has  $K^\pi = 1^-$ .

$$\Phi(3/2^-, -1/2^+) = \mathcal{A}[\phi_1^{(\alpha)}\phi_2^{(\alpha)}(\phi_{c1}\chi_{c1})(\phi_{c2}\chi_{c2})]. \quad (16)$$

$$\phi_{c1}\chi_{c1} = \{(p_x + ip_y)_{+a} + (p_x + ip_y)_{-a}\}|n \uparrow\rangle, \quad (17)$$

$$\phi_{c2}\chi_{c2} = \{(\vec{p})_{+a} - (\vec{p})_{-a}\}|n \downarrow\rangle. \quad (18)$$

This basis state gives  $-47.7$  MeV for  $1^-$  and  $-46.7$  MeV for  $2^-$  at the optimal  $\alpha$ - $\alpha$  distance of 3 fm. This energy splitting between  $1^-$  and  $2^-$  by 1 MeV is much larger than the experimental value of 300 keV (experimentally, the excitation energies of the  $1^-$  state and the  $2^-$  state are 5.96 MeV and 6.26 MeV, respectively). At first, we only examine the tail effect of the valence neutrons with  $S_z = 0$ . We introduce a parameter  $\vec{R}$  for  $\phi_{c2}\chi_{c2}$ , which originally occupies the  $\sigma$ -orbit:

$$\phi_{c2}\chi_{c2} = G_{\vec{R}}|n \downarrow\rangle. \quad (19)$$

However, even if we superpose states with many different positions ( $\vec{R}$ ), the energy splitting between these states is still about 1 MeV ( $1^-$  state is  $-49.9$  MeV and the  $2^-$  state is  $-48.9$  MeV). The employed  $\vec{R}$  values are 0.0, 1.0, 2.0 (fm) for the  $x$ -direction (perpendicular to the  $\alpha$ - $\alpha$  direction) and 0.0, 1.0, 2.0, 3.0, 4.0 (fm) for the  $z$ -direction ( $\alpha$ - $\alpha$  direction).

Therefore, to improve this discrepancy, we next include the basis states with  $S_z = 1$ ;  $\Phi(3/2^-, 1/2^+)$ . The  $S_z = 1$  basis state generates  $K^\pi = 2^-$  band. As a result of the calculation, the energy of the  $2^-$  state with  $K^\pi = 2^-$  (spin triplet) is found to be accidentally



close to the energy of the  $2^-$  state with  $K^\pi = 1^-$  projected from the  $S_z = 0$  basis states. Thus, the coupling effect between the  $S_z = 0$  basis states and the  $S_z = 1$  basis states is larger for the  $2^-$  state than for the  $1^-$  state, and the energy splitting becomes comparable to the experimental one. To see this effect, we superpose many  $S_z = 1$  basis states characterized by the Gaussian center  $\vec{R}$ ;  $\phi_{c2}\chi_{c2} = G_{\vec{R}}|n \downarrow\rangle$ . When we include many states with different  $\vec{R}$  values in our bases states, the energies become  $-51.6$  MeV ( $1^-$ ) and  $-51.2$  MeV ( $2^-$ ). The employed  $\vec{R}$  values are 0.1, 1.0, 2.0 (fm) for the  $x$ -direction and 0.0, 1.0, 2.0, 3.0, 4.0 (fm) for the  $z$ -direction. The experimental small level splitting between  $1^-$  and  $2^-$  is found to be evidence of the spin vibration in the  $2^-$  state.

### C. The structure of $^{12}\text{Be}$

The large contribution of this spin-orbit interaction will be discussed concerning  $^{12}\text{Be}$ . In the previous subsection, we have discussed for  $^{10}\text{Be}$  that this effect is more important as the  $\alpha$ - $\alpha$  becomes smaller, and in  $^{12}\text{Be}$ , we show that the distance is smaller than that of the second  $0^+$  state of  $^{10}\text{Be}$ . In  $^{12}\text{Be}$ , four valence neutrons rotate around two  $\alpha$  clusters and, mainly, two configurations are important for the  $0^+$  ground state [19]. One is  $(3/2^-)^2(1/2^-)^2$  for the four valence neutrons, which corresponds to the closed  $p$ -shell configuration of the neutrons at the zero limit of the  $\alpha$ - $\alpha$  distance. The other configuration is  $(3/2^-)^2(1/2^+)^2$ , where two of the four valence neutrons occupy the  $\sigma$ -orbit. It is necessary to compare the energy of these two configurations as a function of the  $\alpha$ - $\alpha$  distance. The configurations of  $(3/2^-)^2(1/2^-)^2$  and  $(3/2^-)^2(1/2^+)^2$  are constructed as follows:

$$\Phi(3/2^-, -3/2^-, -1/2^-, 1/2^-) = \mathcal{A}[\phi_1^{(\alpha)}\phi_2^{(\alpha)}(\phi_{c1}\chi_{c1})(\phi_{c2}\chi_{c2})(\phi_{c3}\chi_{c3})(\phi_{c4}\chi_{c4})] \quad (20)$$

$$\phi_{c1}\chi_{c1} = \{(p_x + ip_y)_{+a} + (p_x + ip_y)_{-a}\}|n \uparrow\rangle, \quad (21)$$

$$\phi_{c2}\chi_{c2} = \{(p_x - ip_y)_{+a} + (p_x - ip_y)_{-a}\}|n \downarrow\rangle, \quad (22)$$

$$\phi_{c3}\chi_{c3} = \{(p_x - ip_y)_{+a} + (p_x - ip_y)_{-a}\}|n \uparrow\rangle, \quad (23)$$

$$\phi_{c4}\chi_{c4} = \{(p_x + ip_y)_{+a} + (p_x + ip_y)_{-a}\}|n \downarrow\rangle, \quad (24)$$

$$\Phi(3/2^-, -3/2^-, 1/2^+, -1/2^+) = \mathcal{A}[\phi_1^{(\alpha)}\phi_2^{(\alpha)}(\phi_{c1}\chi_{c1})(\phi_{c2}\chi_{c2})(\phi_{c3}\chi_{c3})(\phi_{c4}\chi_{c4})] \quad (25)$$

$$\phi_{c1}\chi_{c1} = \{(p_x + ip_y)_{+a} + (p_x + ip_y)_{-a}\}|n \uparrow\rangle, \quad (26)$$

$$\phi_{c2}\chi_{c2} = \{(p_x - ip_y)_{+a} + (p_x - ip_y)_{-a}\}|n \downarrow\rangle, \quad (27)$$

$$\phi_{c3}\chi_{c3} = \{(\vec{p})_{+a} - (\vec{p})_{-a}\}|n \uparrow\rangle \quad a = d/2, \quad (28)$$

$$\phi_{c4}\chi_{c4} = \{(\vec{p})_{+a} - (\vec{p})_{-a}\}|n \downarrow\rangle \quad a = d/2. \quad (29)$$

The dotted line in Fig. 3 shows  $0^+$  energies of  $(3/2^-)^2(1/2^+)^2$  and the dashed line shows  $(3/2^-)^2(1/2^-)^2$  with respect to the  $\alpha$ - $\alpha$  distance.

---

Fig. 3

---

When the  $\alpha$ - $\alpha$  distance is small, for example 2 fm, the dominant configuration of the four valence neutrons is  $(3/2^-)^2(1/2^-)^2$  for the ground state, which corresponds to the closed  $p$ -shell configuration at the limit of the  $\alpha$ - $\alpha$  distance, zero. On the other hand, the  $(3/2^-)^2(1/2^+)^2$  configuration for the four valence neutrons becomes lower as the  $\alpha$ - $\alpha$  distance is increased. However, it is still higher than the  $(3/2^-)^2(1/2^-)^2$  configuration by a few MeV. Here, we show the importance of the coupling between the  $(3/2^-)^2(1/2^+)^2$  configuration and the spin-triplet state for the last two neutrons ( $(1/2^+)^2$ ). The spin-triplet state for  $(1/2^+)^2$  is introduced as follows:

$$\Phi(3/2^-, -3/2^-, 1/2^+, G_{\vec{R}} | \uparrow) = \mathcal{A}[\phi_1^{(\alpha)} \phi_2^{(\alpha)} (\phi_{c1}\chi_{c1})(\phi_{c2}\chi_{c2})(\phi_{c3}\chi_{c3})(\phi_{c4}\chi_{c4})] \quad (30)$$

$$\phi_{c1}\chi_{c1} = \{(p_x + ip_y)_{+a} + (p_x + ip_y)_{-a}\} |n \uparrow\rangle, \quad (31)$$

$$\phi_{c2}\chi_{c2} = \{(p_x - ip_y)_{+a} + (p_x - ip_y)_{-a}\} |n \downarrow\rangle, \quad (32)$$

$$\phi_{c3}\chi_{c3} = \{(\vec{p})_{+a} - (\vec{p})_{-a}\} |n \uparrow\rangle \quad a = d/2, \quad (33)$$

$$\phi_{c4}\chi_{c4} = G_{\vec{R}} |n \uparrow\rangle. \quad (34)$$

The coupling between the  $(3/2^-)^2(1/2^+)^2$  configuration and the spin-triplet states is shown in Fig. 4 as a function of the parameter  $\vec{R}$ .

---

Fig. 4

---

The point on the  $x$ - $z$  plain in Fig. 4 shows the Gaussian-center  $\vec{R}$  in the spin-triplet state. The contour map shows the energy calculated by taking into account this coupling with the spin-triplet state. This  $\alpha$ - $\alpha$  distance is 3 fm, and this optimal distance is smaller than that for the second  $0^+$  state of  $^{10}\text{Be}$  by about 1 fm, since two of the four valence neutrons occupy the  $(3/2^-)^2$  configuration and increase the binding energy of the system. Because of this effect, the coupling effect of the spin-triplet states is more important than in the case of the second  $0^+$  state of  $^{10}\text{Be}$ . The minimal point of the surface shows that the energy gain due to the couplings is about 4 MeV in  $^{12}\text{Be}$ .

The solid line in Fig. 3 shows the  $0^+$  energy calculated by taking into account the coupling effect between the  $(3/2^-)^2(1/2^+)^2$  configuration and the  $S_z = 0, 1$  basis states for the last two valence neutrons. Due to the spin-orbit coupling, the energy is almost the same as that of  $(3/2^-)^2(1/2^-)^2$  corresponding to the closed  $p$ -shell configuration. Furthermore, the energy of  $(3/2^-)^2(1/2^+)^2$  is suggested to become even lower than  $(3/2^-)^2(1/2^-)^2$  when the pairing effect between  $(3/2^-)^2$  and  $(1/2^-)^2$  is taken into account. These effects plays crucial roles in accounting for breaking of the  $N = 8$  magic number.

## IV. CONCLUSION

The second  $0^+$  state of  $^{10}\text{Be}$  has been shown to be characterized by the  $\sigma$ -orbit of the two valence neutrons in terms of the molecular orbit (MO) model. The two valence neutrons stay along the  $\alpha$ - $\alpha$  axis (the  $1/2^+$  orbit) and reduce the kinetic energy by enlarging the  $\alpha$ - $\alpha$  distance. This simple description for the second  $0^+$  state gives a higher excitation energy by 5 MeV compared to the experimental one. To improve the description, spin-triplet basis states which have not been included in the traditional MO models are prepared by allowing a deviation of the neutron orbit from one just along the  $\alpha$ - $\alpha$  axis. Thus, the spin-orbit interaction can be taken into account, and the calculated second  $0^+$  state becomes lower by 3.5 MeV. The precise description of the neutron-tail also decreases the excitation energy by 1.5 MeV. The discrepancy between the experimental excitation energy and the calculated one is compensated by these two effects.

The spin-mixing effects were studied for the negative parity state of  $^{10}\text{Be}$ . If we restrict ourselves to the  $S_z = 0$  basis state, this energy splitting between the  $1^-$  state and  $2^-$  state is about 1 MeV, which is much larger than the experimental value of 303 keV. As a result of adding basis states with  $S_z = 1$ , where the spin directions of the two valence neutrons are the same, the  $K$ -mixing occurs especially for the  $2^-$  state. The contribution of the  $S_z = 1$  state is larger for the  $2^-$  state. The resultant energy splitting becomes comparable to the experimental one. Therefore, the experimental small level splitting between  $1^-$  and  $2^-$  is considered to be a result of the spin vibration induced by the spin-orbit interaction in the  $2^-$  state.

The coupling with the spin-triplet basis states is also important in the case of  $^{12}\text{Be}$ . Without the spin-triplet basis state, the energy of the configuration  $(3/2^-)^2(1/2^+)^2$  is much higher than that of the closed  $p$ -shell configuration  $((3/2^-)^2(1/2^-)^2)$  by 4 MeV. However, the energy of  $(3/2^-)^2(1/2^+)^2$  is drastically decreased by coupling with the spin-triplet states. This is because the effect becomes stronger as the  $\alpha$ - $\alpha$  distance becomes shorter, and  $^{12}\text{Be}$  has an optimal  $\alpha$ - $\alpha$  distance around 3 fm, which is smaller than the second  $0^+$  state of  $^{10}\text{Be}$  by 1 fm. The study shows that an energy of  $(3/2^-)^2(1/2^+)^2$  is almost the same as  $(3/2^-)^2(1/2^-)^2$ , or even lower. This effect is suggested to play a crucial role in accounting for the dissipation of the  $N = 8$  magic number in  $^{12}\text{Be}$ . It is an interesting subject to analyze the binding mechanism and properties of the ground state by taking into account the pairing mixing among states with configurations of  $(3/2^-)^2(1/2^-)^2$ ,  $(3/2^-)^2(1/2^+)^2$ , and  $(1/2^-)^2(1/2^+)^2$ . A detail analysis is going to be performed not only for this state, but also for excited states where new states with cluster structure have been recently observed.

## ACKNOWLEDGMENTS

The authors would like to thank Prof. I. Tanihata for various effective suggestions. They also thank other members of RI beam science laboratory in RIKEN for discussions and encouragements. One of the authors (N.I) thanks fruitful discussions with Prof. R. Lovas, Prof. H. Horiuchi, Prof. T. Otsuka, Prof. Y. Abe, Prof. K. Katō, Prof. K. Yabana, Dr. A. Ohnishi, and Dr. Y. Kanada-En'yo.

## REFERENCES

- [1] I. Tanihata, T. Kobayashi, O. Yamakawa, S. Shimoura, K. Ekuni, K. Sugimoto, N. Takahashi, T. Shimoda, and H. Sato  
Phys.Lett. B206, 592 (1988).
- [2] *Proc. of Int.Symp.on Phys. of Unstable Nuclei, Niigata* Nucl.Phys. A588 1 (1995)  
*Proc. of Fourth Int.Conf.on Radioactive Nuclear Beam, Omiya* Nucl.Phys. A616 1 (1997)
- [3] I. Tanihata, J.Phys. G: Nucl.Part.Phys. **22**, 157 (1996).
- [4] T. Suzuki and T. Otsuka Phys. Rev. C**56**, 847 (1997). 279 (1992).
- [5] S. Okabe, Y. Abe, and H. Tanaka Prog.Theor.Phys. 57, 866 (1977).  
S. Okabe and Y. Abe Prog.Theor.Phys. 59, 315 (1978).
- [6] S. Okabe and Y. Abe, Prog.Theor.Phys. 61, 1049 (1979).
- [7] H. Furutani, H. Kanada, T. Kaneko, S. Nagata, H. Nishioka, S. Okabe S. Saito, T. Sakuda, and M. Seya, Prog. Theor. Phys. Suppl. 68, 193 (1980).
- [8] M. Seya, M. Kohno, and S. Nagata, Prog. Theor. Phys. 65, 204 (1981).
- [9] N. Itagaki, S. Okabe, Physical Review C**61** 044306 (2000)
- [10] Y. Abe J. Hiura, and H. Tanaka, Prog.Theor.Phys.**49**, 800 (1973).
- [11] A.B. Volkov Nucl. Phys. 74, 33 (1965).
- [12] N. Yamaguchi, T. Kasahara, S. Nagata and Y. Akaishi, Prog.Theor.Phys. 62 1018 (1979)
- [13] Y. Kanada-En'yo and H. Horiuchi, Prog. Theor. Phys. 93, 115 (1995).
- [14] Y. Kanada-En'yo, H. Horiuchi and A. Ono, Phys. Rev. C52, 628 (1995).
- [15] Y. Kanada-En'yo and H. Horiuchi Phys. Rev. C52, 647 (1995).
- [16] A.Doté, H. Horiuchi and Y. Kanada-En'yo, Phys. Rev. C**56**, 1844 (1997).
- [17] A. Ono, H. Horiuchi, T. Maruyama and A. Ohnishi,  
Prog.Theor.Phys. 87 1185, (1992); Phys.Rev.Lett.68 2898, (1992).
- [18] F. Ajzenberg-Selove, Nucl.Phys. A490, 1 (1988).
- [19] N. Itagaki and S. Okabe, *Proceedings of 7<sup>th</sup> International Conference on Clustering Aspects of Nuclear Structure and Dynamics* (Rab, Croatia, 1999)

## FIGURES

FIG. 1. The  $0^+$  energy curve for  $\Phi(3/2^-, -3/2^-)$ ,  $\Phi(1/2^-, -1/2^-)$ , and  $\Phi(1/2^+, -1/2^+)$  as a function of the  $\alpha$ - $\alpha$  distance ( $d$ ).

FIG. 2. The energy surface of the second  $0^+$  state of  $^{10}\text{Be}$ . The total energy including the coupling effect between the  $(1/2^+)^2$  configuration and the spin-triplet configuration is shown. The  $\alpha$ - $\alpha$  distance is optimal 4 fm, and the spheres show  $\alpha$  clusters. The axes (fm) show the position of the Gaussian-center of one valence neutron in the spin-triplet state which deviates from the  $\sigma$ -orbit.

FIG. 3. The energy surface of the ground state of  $^{12}\text{Be}$ . The total energy including the coupling effect between the  $(3/2^-)^2(1/2^+)^2$  configuration and the spin-triplet configuration for the last two valence neutrons is shown. The  $\alpha$ - $\alpha$  distance is optimal 3 fm, and the spheres show  $\alpha$  clusters. The axes (fm) show the position of the Gaussian-center of one valence neutron in the spin-triplet state which deviates from the  $\sigma$ -orbit

FIG. 4. The  $0^+$  energies for  $(3/2^-)^2(1/2^+)^2$  configuration (dotted line) and  $(3/2^-)^2(1/2^-)^2$  configuration (dashed line) in  $^{12}\text{Be}$ . In the solid line, the couplings among the  $(3/2^-)^2(1/2^+)^2$  configuration, an optimal  $S_z = 1$  state, and  $S_z = 0$  states are included. The resultant state almost degenerates with the  $(3/2^-)^2(1/2^-)^2$  configuration.

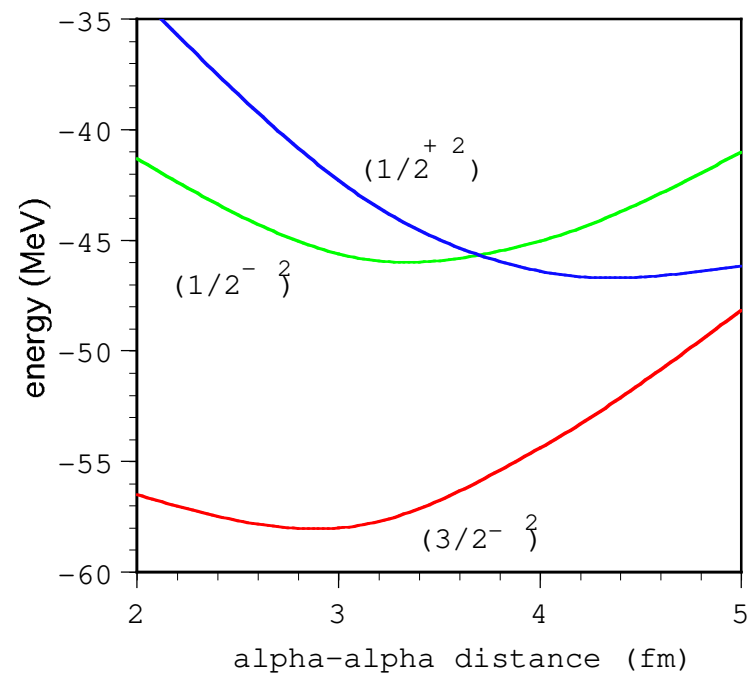
## TABLES

TABLE I. The energy convergence of the second  $0^+$  of  $^{10}\text{Be}$ . The  $\alpha$ - $\alpha$  distance is fixed to 4 fm. The row noted as  $\Phi(1/2^+, -1/2^+)$  shows the energy of the  $\Phi(1/2^+, -1/2^+)$  configuration, and the row  $S = 0 (\sigma)^2$  shows the energy when a linear combination of local Gaussians is optimized. The row spin-orbit shows the energy including the coupling with the spin-triplet state. The row tail shows the calculated energy when the tail of the valence neutron is further expressed by the  $S_z = 0$  basis states. The values in parentheses give the energy difference with the previous row.

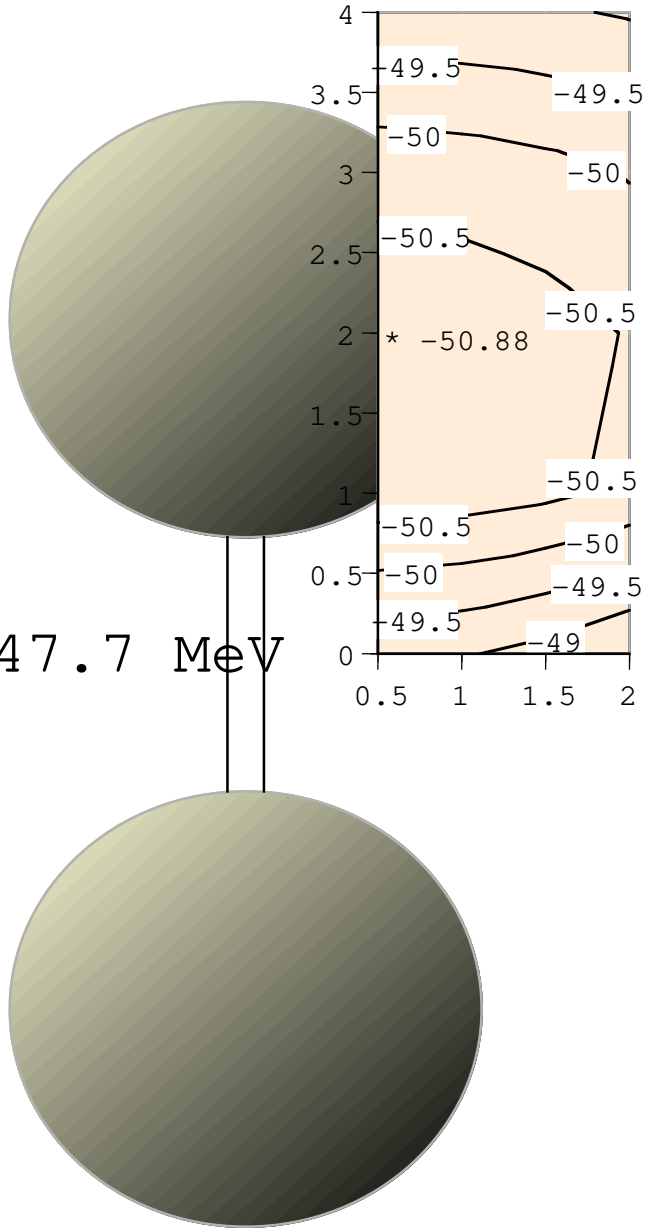
	number of Gaussians for one valence neutron	$0^+$ energy
$\Phi(1/2^+, -1/2^+)$	4	-46.3
$S = 0 (\sigma)^2$	4	-47.7 (-1.4)
spin-orbit	24	-51.2 (-3.5)
tail	44	-52.9 (-1.7)

TABLE II. The second  $0^+$  energy of  $^{10}\text{Be}$  for each  $\alpha$ - $\alpha$  distance. The row  $S = 0 (\sigma)^2$  shows the energy of the  $\Phi(1/2^+, -1/2^+)$  configuration, where a linear combination of local Gaussians is optimized. The row  $+S_z = 1$  represents the energy including the coupling between  $S = 0 (\sigma)^2$  and the spin-triplet state. The row  $+S_z = 0, 1$  represents the energy including the coupling between  $S = 0 (\sigma)^2$  and both the spin-singlet and the spin-triplet states. The values in parentheses give the energy difference with the  $S = 0$  state.

$\alpha$ - $\alpha$ distance (fm)	$S = 0 (\sigma)^2$ (MeV)	$+S_z = 1$ (MeV)	$+S_z = 0, 1$ (MeV)
3	-44.5	-48.9 (-4.4)	-50.6 (-6.1)
4	-47.7	-51.2 (-3.5)	-52.9 (-5.0)
5	-46.9	-50.0 (-3.1)	-51.5 (-4.6)



<sup>2</sup>  
(sigma) -47.7 MeV





(sigma)<sup>2</sup>

-53.3 MeV

